Resveratrol improves palmitic acid-induced insulin resistance via the DDIT4/mTOR pathway in C2C12 cells

XINYAN PAN[1,2], CHUNQIAO LIU[2], XING WANG[2], MING ZHAO[3], ZHIMEI ZHANG[1], XUEMEI ZHANG[4], CHAO WANG[2] and GUANGYAO SONG[1,2]

[1]Department of Endocrinology; [2]Hebei Key Laboratory of Metabolic Diseases; [3]Clinical Laboratory and [4]Department of Rheumatism and Immunology, Hebei General Hospital, Shijiazhuang, Hebei 050051, P.R. China

Received February 9, 2023; Accepted July 19, 2023

DOI: 10.3892/mmr.2023.13068

Abstract. The present study aimed to establish a model of palmitic acid (PA)-induced insulin resistance (IR) in C2C12 cells and to determine the mechanism underlying how resveratrol (RSV) improves IR. C2C12 cells were divided into the control (CON), PA, PA + RSV, PA + RSV + DNA damage-inducible transcript 4 (DDIT4)-small interfering (si)RNA and PA + RSV + MHY1485 (mTOR agonist) groups. Glucose contents in culture medium and triglyceride contents in cells were determined. Oil red O staining was performed to observe the pathological changes in the cells. Reverse transcription-quantitative PCR and western blotting were conducted to evaluate the mRNA and protein expression levels, respectively, of DDIT4, mTOR, p70 ribosomal protein S6 kinase (p70S6K), insulin receptor substrate (IRS)-1, PI3K, AKT and glucose transporter 4 (GLUT4). Compared with in the CON group, glucose uptake was decreased, cellular lipid deposition was increased, phosphorylated (p)-IRS-1, p-mTOR and p-p70S6K protein expression levels were increased, and p-PI3K, p-AKT, GLUT4 and DDIT4 protein expression levels were decreased in the PA group. By contrast, compared with in the PA group, culture medium glucose content and cellular lipid deposition were decreased, p-PI3K, p-AKT, GLUT4 and DDIT4 protein expression levels were increased, p-IRS-1 protein expression levels were decreased, and mTOR and p70S6K mRNA and protein expression levels were decreased in the PA + RSV group. Compared with in the PA + RSV group, DDIT4 protein and mRNA expression levels were reduced in the PA + RSV + DDIT4-siRNA group, but showed no change in the PA + RSV + MHY1485 group. Following transfection with DDIT4-siRNA or treatment with MHY1485, the effects of RSV on improving IR and lipid metabolism were weakened, mTOR and p70S6K protein expression levels were upregulated, p-PI3K, p-AKT and GLUT4 protein expression levels were down-regulated, p-IRS-1 protein expression levels were upregulated, and culture medium glucose content and cellular lipid deposition were increased. In conclusion, RSV may improve PA-induced IR in C2C12 cells through the DDIT4/mTOR/IRS-1/PI3K/AKT/GLUT4 signaling pathway, as well as via improvements in glucose and lipid metabolism.

Introduction

Insulin resistance (IR) is one of the main features of type 2 diabetes mellitus and is closely related to lipid metabolism disorders (1-3). Skeletal muscle accounts for 75-80% of systemic glucose uptake in the body and has an important role in IR (4,5).

Resveratrol (RSV) is a polyphenolic phytoalexin mainly derived from peanuts, grapes, knotweed, mulberries and other plants (6). It has beneficial effects on metabolism, and can improve IR and other metabolic abnormalities, including dyslipidemia, hyperglycemia and hyperinsulinemia (7). Among these properties, the anti-IR effect of RSV has been confirmed in a number of studies (8,9). A previous *in vitro* study has demonstrated that RSV can stimulate glucose uptake in skeletal muscle cells (10), and an *in vivo* study has shown that RSV significantly improves insulin sensitivity in mice fed a high-fat diet (11). Although several studies have investigated the antidiabetic effects of RSV (12,13), the underlying mechanism for its effects against IR has not been fully elucidated.

mTOR has been implicated in various human diseases and pathological states, including diabetes, obesity, cancer and neurodegenerative diseases (14-17). The main downstream target of mTOR is p70 ribosomal protein S6 kinase (p70S6K) (18). Notably, it has been reported that the mTOR signaling pathway can be activated by energy overload, leading to the occurrence of IR (19).

DNA damage-inducible transcript 4 (DDIT4; also known as Redd1, RTP801 and Dig2) functions in DNA damage repair, insulin signaling, oxidative metabolism, nutrient deprivation,

Correspondence to: Professor Guangyao Song, Hebei Key Laboratory of Metabolic Diseases, Hebei General Hospital, 348 Heping West Road, Shijiazhuang, Hebei 050051, P.R. China
E-mail: sguangyao2@163.com

Abbreviations: RSV, resveratrol; IR, insulin resistance; PA, palmitic acid; DDIT4, DNA damage-inducible transcript 4; p70S6K, p70 ribosomal protein S6 kinase; IRS-1, insulin receptor substrate-1; GLUT4, glucose transporter 4; TG, triglyceride

Key words: RSV, IR, PI3K, AKT, GLUT4, DDIT4, mTOR, p70S6K

hypoxia and endoplasmic reticulum stress, which can negatively regulate mTOR activity (20-23). DDIT4 and mTOR are also involved in regulation of the adipocyte insulin signaling pathway (24). However, the mechanisms underlying the effects of DDIT4 and mTOR on skeletal muscle IR remain to be fully elucidated. The possibility that RSV may regulate skeletal muscle IR via the DDIT4/mTOR pathway warrants further research to identify new targets for RSV in the improvement of IR.

To investigate the underlying mechanism for how RSV improves IR, the present study established a palmitic acid (PA)-induced IR model in C2C12 cells, verified the effects of RSV on PA-induced IR, and glucose and lipid metabolism in the model, and explored whether the effects of RSV were related to the DDIT4/mTOR signaling pathway.

Materials and methods

C2C12 cell culture and treatments. The C2C12 mouse myoblast cell line (cat. no. CL-0044) was obtained from Procell Life Science & Technology Co., Ltd. C2C12 cells were maintained in DMEM (cat. no. C11995500BT; Gibco; Thermo Fisher Scientific, Inc.) supplemented with 10% fetal bovine serum (cat. no. FSP500; Shanghai ExCell Biology, Inc.) and 1% penicillin/streptomycin (cat. no. P1400; Beijing Solarbio Science & Technology Co., Ltd.) at 37˚C under 5% CO_2. After the cells reached 70-80% confluence, cell differentiation was induced by culture in DMEM supplemented with 2% horse serum (cat. no. S9050; Beijing Solarbio Science & Technology Co., Ltd.) and 1% penicillin/streptomycin. Mycoplasma contamination was not detected in the cells. Differentiated C2C12 cells at a density of $1x10^4$ cells/cm^2 were then incubated with 0.1 mM (PA1 group), 0.25 mM (PA2 group) or 0.5 mM (PA3 group) PA (cat. no. P0500; Sigma-Aldrich; Merck KGaA) at room temperature for 24 h. A total of 0, 12 and 24 h after the addition of PA (0.1, 0.25 or 0.5 mM), the glucose concentration in the culture medium was measured using the Glucose Oxidase Assay Kit (cat. no. E1011; Beijing Applygen Technologies, Inc.) to determine whether IR was established in the cells. The optimal concentration of PA was selected by measuring the cellular triglyceride (TG) content, number of Oil red O-stained droplets, and the protein and mRNA expression levels of insulin pathway indicators in the PA1, PA2 and PA3 groups.

When the cells reached ~80% confluence, RSV (cat. no. RS-BLLC; Hangzhou Great Forest Biomedical Ltd.) was added to the medium at concentrations of 10, 20, 30, 50 and 100 μM at room temperature. After 24 h, 10 μl Cell Counting Kit-8 (cat. no. CK04; Dojindo Laboratories, Inc.) was added to each well and incubated at 37˚C for 20 min, before the absorbance was measured at 450 nm. Cell survival rate was calculated as follows: Cell survival rate (%)=[(As-Ab)/(Ac-Ab)] x100; where As indicates the OD value of culture medium containing cells treated with different concentrations of RSV; Ac indicates the OD value of culture medium containing untreated cells; and Ab indicates the OD value of culture medium containing no cells. The cell survival rate was calculated to select the appropriate RSV concentration for subsequent experiments.

In addition, C2C12 cells were treated with 10 μM MHY1485 (mTOR agonist) (cat. no. A01B013361; Energy Chemical Co., Ltd.) and transfected with a small interfering (si)RNA against DDIT4 (DDIT4-siRNA) (Shanghai Genechem Co. Ltd.) at 37˚C for 24 h. The cells were divided into the following groups: The control (CON) group; PA (0.5 mM) group; PA (0.5 mM) + RSV (30 μM) group; PA (0.5 mM) + RSV (30 μM) + DDIT4-siRNA group; and PA (0.5 mM) + RSV (30 μM) + MHY1485 (10 μM) group. All cells were treated with 100 nM insulin (Sigma-Aldrich; Merck KGaA) for 30 min at 37˚C before western blotting and detection of glucose contents in order to stimulate the phosphorylation of indicators (IRS-1/PI3K/AKT) in the insulin signaling pathway. The cells were collected for western blotting and reverse transcription-quantitative PCR (RT-qPCR) analyses.

Detection of glucose contents in culture medium. After stimulation with insulin for 30 min, the glucose oxidase-peroxidase method was employed to measure the concentration of glucose remaining in the culture medium at 0, 12 and 24 h using the Glucose Oxidase Assay Kit. Briefly, 8 ml reagent R1 and 2 ml reagent R2 in a 4:1 ratio were mixed to prepare 10 ml working solution. Subsequently, 5 μl culture medium and 1 ml working solution were mixed in test tubes, and blank and standard tubes were also set up. The absorbance of each tube was measured at 450 nm and was used to calculate the residual glucose concentration in the culture medium.

TG assay. The concentrations of TG in the cultured cells at a density of $5x10^5$ cells/cm^2 were measured using a commercially available Triglyceride Assay Kit (cat. no. A110-1-1; Nanjing Jiancheng Biological Engineering Research Institute) in accordance with the manufacturer's instructions.

Oil red O staining to observe lipid droplets in the cytoplasm of C2C12 cells. An Oil Red O Stain Kit (cat. no. G1262; Beijing Solarbio Science & Technology Co., Ltd.) was used to detect lipid droplets in the cytoplasm of C2C12 cells. C2C12 cells were cultured in 6-well plates and the medium was discarded. The cells were then stained with filtered Oil red O solution at room temperature for 15 min, rinsed with 37˚C water for 20 sec, stained with counterstain solution for 3 min, rinsed with 37˚C water for 5 sec, and covered with curing agent. The lipid droplets in the cell cytoplasm were observed under a light microscope (TS100F; Nikon Corporation) at x400 magnification. In addition, the lipid deposition in cells was semi-quantified using ImageJ software (version 1.8.0; National Institutes of Health) (25).

Transfection with siRNAs. Three DDIT4-siRNAs (5'-GGG AAGGAAGUGUUCUCCAGGAAGU-3'; 5'-GCAGCTGCT CATTGA AGAGTGTTGA-3'; 5'-GGTGCCCATGTACTG GAGGATTCAA-3') and a negative control siRNA (5'-CCU CUUACCUCAGUUACA AUUUAUA-3') sequence were purchased from Shanghai Genechem Co., Ltd. For preparation, 50 μl Opti-MEM I reduced serum medium (cat. no. 31985-062; Thermo Fisher Scientific, Inc.) was added to 20 pmol siRNA to obtain a RNA oligonucleotide stock solution, which was stored at -20˚C. Furthermore, 50 μl Opti-MEM I medium was used to dilute 1 μl Lipofectamine® 2000 (cat. no. 11668; Invitrogen; Thermo Fisher Scientific, Inc.). For experiments, the RNA oligonucleotide stock solution and the diluted Lipofectamine 2000 solution were mixed to prepare transfection complexes

at room temperature. Cells were seeded into 24-well plates once they reached ~40% confluence at 37˚C. Transfection was performed when the cells reached ~60% confluence, with 100 μl siRNA transfection complexes at a concentration of 50 nM added to each well and incubated at 37˚C for 24 h. The transfection efficiency of the different siRNAs was examined by western blotting 24 h post-transfection to select the optimal siRNA for use in subsequent experiments. The optimal sequence of the DDIT4-siRNA was: 5'-GGGAAGGAAGUG UUCUCCAGGAAGU-3'.

RT-qPCR. Total RNA was extracted from cultured cells using an RNAsimple Total RNA Kit (cat. no. DP419; Tiangen Biotech Co., Ltd.), and its purity and concentration were determined using a NanoDrop® 2000 (Thermo Fisher Scientific, Inc.). Subsequently, RNA was reverse transcribed into cDNA using a PrimeScript™ RT Reagent Kit (cat. no. RR047A; Takara Biotechnology Co., Ltd.) according to the manufacturer's protocol. Amplification was performed using a SYBR® Premix Ex Taq™ II Kit (cat. no. RR820A; Takara Biotechnology Co., Ltd.) in an Applied Biosystems 7500 Real-Time PCR System (Thermo Fisher Scientific, Inc.). The cycling conditions were as follows: 3 min of predenaturation at 95˚C, followed by 40 cycles at 95˚C for 5 sec and 60˚C for 32 sec, and the fluorescence was detected at the end of each cycle. The mRNA expression levels of insulin receptor substrate (IRS)-1, PI3K, AKT, glucose transporter 4 (GLUT4), DDIT4, mTOR and p70S6K were evaluated in the cultured cells. β-actin was measured as an internal control. The relative mRNA expression levels were quantified using the $2^{-\Delta\Delta Cq}$ method (26). The sequences of the primers used in the present study are listed in Table I.

Table I. Primer sequences.

Gene	Sequence, 5'-3'
DDIT4	F: TACTGCCCACCTTTCAGTTG
	R: GTCAGGGACTGGCTGTAACC
mTOR	F: GCGGCCTGGAAATGCGGAAGTGG
	R: AAAGCCCCAAGGAGCCCCAACA
p70S6K	F: CACTCAGGCCCCCCTACACT
	R: GCCGTCACTGAAAACCAAGTTC
PI3K	F: CCCATGGGACAACATTCCAA
	R: CATGGCGACAAGCTCGGTA
AKT	F: TCAGGATGTGGATCAGCGAGA
	R: CTGCAGGCAGCGGATGATAA
IRS-1	F: GCACCTGGTGGCTCTCTACAC
	R: TCGCTATCCGCGGCAAT
GLUT4	F: GTGACTGGAACACTGGTCCTA
	R: CCAGCCACGTTGCATTGTAG
β-actin	F: GGTGGGAATGGGTCAGAAGG
	R: AGGTCTCAAACATGATCTGGGT

F, forward; R, reverse; DDIT4, DNA damage-inducible transcript 4; p70S6K, p70 ribosomal protein S6 kinase; IRS-1, insulin receptor substrate-1; GLUT4, glucose transporter 4.

Western blotting. C2C12 cells were collected after culture and treatment, and lysed in RIPA lysis buffer (cat. no. R0010; Beijing Solarbio Science & Technology Co., Ltd.). The lysed cells were scraped off using a cell scraper, solubilized in 3X SDS sample buffer (cat. no. P1040; Beijing Solarbio Science & Technology Co., Ltd.) and the protein concentration was determined using a BCA kit (cat. no. 23225; Thermo Fisher Scientific, Inc.). Total proteins (30 μg) were separated by SDS-PAGE on 10% gels and were transferred to polyvinylidene fluoride membranes (cat. no. ISEQ00010; MilliporeSigma.), which were blocked with 5% skimmed milk at room temperature for 2 h. The membranes were then incubated with the following primary antibodies at 4˚C overnight: Total (t)-IRS-1 (cat. no. ab52167; Abcam), rabbit antibody, 1:1,000; phosphorylated (p)-IRS-1 (cat. no. ab5599; Abcam), rabbit antibody, 1:1,000; t-AKT (cat. no. BS2987; Bioworld Technology, Inc.), rabbit antibody, 1:2,000; p-AKT (cat. no. BS4006; Bioworld Technology, Inc.), rabbit antibody, 1:2,000; t-PI3K (cat. no. 20583-1-AP; Proteintech Group, Inc.), rabbit antibody, 1:2,000; p-PI3K (cat. no. 11508; SAB Biotherapeutics, Inc.), rabbit antibody, 1:2,000; GLUT4 (cat. no. ab65267; Abcam), mouse antibody, 1:2,000; DDIT4 (cat. no. ab106356; Abcam), rabbit antibody, 1:2,000; t-mTOR (cat. no. ab32028; Abcam), rabbit antibody, 1:1,000; p-mTOR (cat. no. ab109268; Abcam), rabbit antibody, 1:1,000; t-p70S6K (cat. no. ab32529; Abcam), rabbit antibody, 1:1,000; p-p70S6K (cat. no. ab59208; Abcam), rabbit antibody, 1:1,000; β-actin (cat. no. 20536-1-AP; Proteintech Group, Inc.), mouse antibody, 1:5,000. After three washes with Tris-buffered saline containing 20% Tween-20, the membranes were incubated with appropriate horseradish peroxidase-conjugated secondary antibodies for 2 h at room temperature as follows: Anti-rabbit (cat. no. S0001; Affinity Biosciences), 1:8,000; anti-mouse (cat. no. S0002; Affinity Biosciences), 1:8,000. The membranes were washed and immersed in chemiluminescence solution (cat. no. 34580; Thermo Fisher Scientific Inc.) for ~2 min, and images of the target bands were acquired using a Gel Imager System (GDS8000; Analytik Jena AG). ImageJ software version 1.8.0 was used to measure the optical densities of the target bands.

Statistical analysis. Statistical analyses were conducted using SPSS 23.0 software (IBM Corp.). All samples were run in triplicate. All data are expressed as the mean ± SD. The mean values of multiple samples were compared by one-way analysis of variance followed by Bonferroni's multiple comparison test or Tamhane's multiple comparison test when there were unequal variances. $P<0.05$ was considered to indicate a statistically significant difference.

Results

Establishment of a PA-induced IR model in C2C12 cells. As shown in Fig. 1A, C2C12 cells were treated with PA at different concentrations (0.1, 0.25 or 0.5 mM). After 12 h, the glucose concentration in the culture medium from the PA3 group (0.5 mM PA) was significantly higher than that from the CON group. After 24 h, the glucose concentrations in the culture media from both the PA2 (0.25 mM PA) and PA3 groups were significantly higher than that from the CON group.

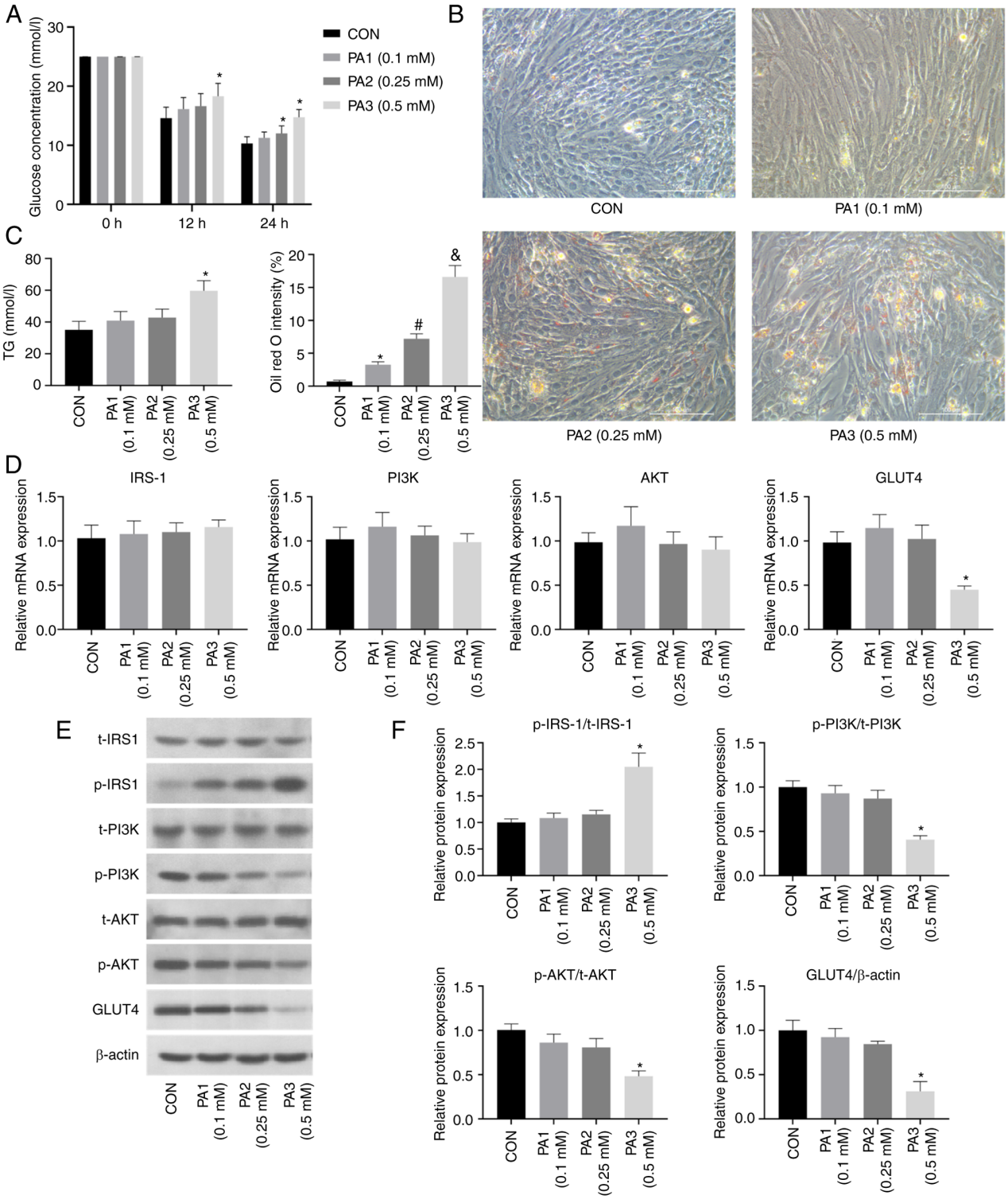

Figure 1. PA induces lipid deposition and insulin resistance in C2C12 cells. (A) Glucose concentration in the culture medium was increased after PA treatment for 24 h. (B) Oil red O staining of C2C12 cells revealed lipid deposition 24 h after PA treatment; magnification, x400, scale bar, 100 μm. (C) TG content was increased in C2C12 cells after PA treatment. (D) Effects of PA treatment on the mRNA expression levels of insulin pathway indicators (IRS-1, PI3K, AKT and GLUT4) in C2C12 cells. (E) Effects of PA treatment on the protein expression levels of insulin pathway indicators in C2C12 cells. (F) Semi-quantification of p-protein/t-protein ratios for insulin pathway indicators (IRS-1, PI3K, AKT) and protein expression levels of GLUT4 in C2C12 cells after PA treatment. All cells were treated with 100 nM insulin for 30 min before (A) detection of glucose contents and (E) western blotting. Data are presented as the mean ± SD (n=3). *P<0.05 vs. CON, $^{\#}$P<0.05 vs. PA1 (0.1 mM), $^{\&}$P<0.05 vs. PA2 (0.25 mM). CON, control; PA, palmitic acid; IRS-1, insulin receptor substrate-1; GLUT4, glucose transporter 4; p-, phosphorylated; t-t, total; TG, triglyceride.

As determined by Oil red O staining, a light blue cytoplasm was observed in the CON group, whereas orange-red lipid droplets were present in the PA1, PA2 and PA3 groups, and the PA3 group had the largest number of droplets (Fig. 1B). The cellular TG contents in the PA1, PA2 and PA3 groups were increased compared with those in the CON group, and

the PA3 group had the highest TG content (Fig. 1C). Based on these findings, the concentration of 0.5 mM PA was selected for subsequent experiments.

As shown in Fig. 1D, compared with those in the CON group, the mRNA expression levels of GLUT4 were significantly decreased in the PA3 group, but unchanged in the PA1 and PA2 groups. Notably, the mRNA expression levels of IRS-1, PI3K and Akt remained unchanged in the PA-treated groups.

As shown in Fig. 1E and F, compared with those in the CON group, the protein expression levels of p-PI3K/t-PI3K, p-AKT/t-AKT and GLUT4 were decreased in the PA3 group, whereas the protein expression levels of p-IRS-1/t-IRS-1 were increased. In the PA1 and PA2 groups, the protein expression levels of p-IRS-1/t-IRS-1, p-PI3K/t-PI3K, p-AKT/t-AKT and GLUT4 were unchanged compared with those in the CON group. Notably, there were no significant differences in the total protein expression levels of IRS-1, PI3K and AKT among the groups. These results confirmed that 0.5 mM PA inhibited the insulin pathway in C2C12 cells, indicating successful establishment of an IR model in C2C12 cells.

RSV improves PA-induced lipid deposition and IR in C2C12 cells. The viability of C2C12 cells was measured following treatment with 0.5 mM PA and RSV at concentrations of 10, 20, 30, 50 or 100 μM for 24 h (Fig. 2A). No difference in cell viability was observed between the 0.5 mM PA group and the CON group. Treatment with RSV at 50 and 100 μM significantly reduced cell viability, whereas treatment with RSV at 10, 20 and 30 μM did not. Therefore, a concentration of 30 μM RSV was selected for subsequent experiments to observe the effects of RSV on PA-treated cells.

The C2C12 cells were grouped into the CON group, PA (0.5 mM) group and PA (0.5 mM) + RSV (30 μM) group. Compared with that in the PA group, the glucose level in the culture medium was decreased in the PA + RSV group (Fig. 2B). These results indicated that RSV may increase insulin-stimulated glucose uptake, promote glucose utilization by cells and reduce gluconeogenesis.

Oil red O staining revealed that the number of cytoplasmic orange-red lipid droplets in the PA + RSV group was lower than that in the PA group (Fig. 2C). Furthermore, the cellular TG content in the PA + RSV group was significantly lower than that in the PA group (Fig. 2D). These results suggested that RSV improved the lipid deposition in C2C12 cells induced by PA treatment.

There were no differences in the mRNA expression levels of IRS-1, PI3K and AKT among the three groups. By contrast, the mRNA expression levels of GLUT4 were decreased in the PA group compared with those in the CON group, but were increased in the PA + RSV group compared with those in the PA group (Fig. 2E).

The total protein expression levels of IRS-1, PI3K and AKT were not significantly affected by treatment with PA or RSV. However, compared with those in the CON group, the protein expression levels of p-PI3K/t-PI3K, p-AKT/t-AKT and GLUT4 were decreased, whereas those of p-IRS-1/t-IRS-1 were increased in the PA group (Fig. 2F and G). Compared with those in the PA group, the protein expression levels of p-PI3K/t-PI3K, p-AKT/t-AKT and GLUT4 were increased, whereas those of p-IRS-1/t-IRS-1 were decreased in the PA + RSV group (Fig. 2F and G). These results suggested that RSV may have a beneficial role in the insulin signaling pathway and could reverse PA-induced IR in C2C12 cells.

Effects of RSV on PA-induced expression of DDIT4 and mTOR pathway components in C2C12 cells. Compared with those in the CON group, the mRNA and protein expression levels of DDIT4 were significantly decreased in the PA group, indicating that PA may cause a decrease in DDIT4 expression. Compared with those in the PA group, the DDIT4 mRNA and protein expression levels were increased in the PA + RSV group, indicating that RSV may promote the expression of DDIT4 (Fig. 3A and B). By contrast, the mRNA expression levels of mTOR and p70S6K were significantly increased in the PA group compared with those in the CON group, but were significantly decreased in the PA + RSV group compared with those in the PA group (Fig. 3C).

In the PA group, compared with in the CON group, the t-protein and p-protein expression levels of mTOR and p70S6K were markedly increased (Fig. 3D), and the p-protein/t-protein ratios for mTOR and p70S6K were also significantly increased (Fig. 3E). In the PA + RSV group, compared with in the PA group, the t-protein and p-protein expression levels of mTOR and P70S6K were markedly decreased (Fig. 3D), and the p-protein/t-protein ratios for mTOR and p70S6K were also decreased (Fig. 3E). These findings indicated that RSV weakened the effects of PA and inhibited the mTOR pathway.

Expression of insulin signaling pathway-related and mTOR pathway-related indicators after silencing of DDIT4. Three siRNAs targeting DDIT4 were used in the present study to verify the effect on DDIT4 silencing. The protein expression levels of DDIT4 in the three transfection groups were significantly lower than those in the negative control group. Notably, DDIT4-siRNA-1 had the most significant silencing effect and was thus selected for subsequent experiments (Fig. 4A). The cells were grouped as follows: CON, PA, PA + RSV and PA + RSV + DDIT4-siRNA groups.

In the PA + RSV + DDIT4-siRNA group, compared with in the PA + RSV group, the glucose concentration was significantly increased in the culture medium, and the effects of RSV on promoting utilization of cellular glucose and reducing gluconeogenesis were weakened (Fig. 4B). These findings indicated that RSV promoted glucose uptake via DDIT4. Furthermore, compared with in the PA + RSV group, the Oil red O staining and TG content measurement results revealed increases in the number of intracellular lipid droplets and cellular TG content in the PA + RSV + DDIT4-siRNA group after silencing of DDIT4, which offset the effect of RSV on reducing cell lipid deposition (Fig. 4C and D). These findings indicated that RSV was effective for improving cellular lipid deposition through DDIT4.

Compared with in the PA + RSV group, the mRNA and protein expression levels of DDIT4 were significantly decreased in the PA + RSV + DDIT4-siRNA group, indicating that the silencing effect on DDIT4 was significant (Fig. 4E-G).

In the PA + RSV + DDIT4-siRNA group, the t-protein and p-protein expression levels of mTOR and p70S6K were increased compared with those in the PA + RSV group

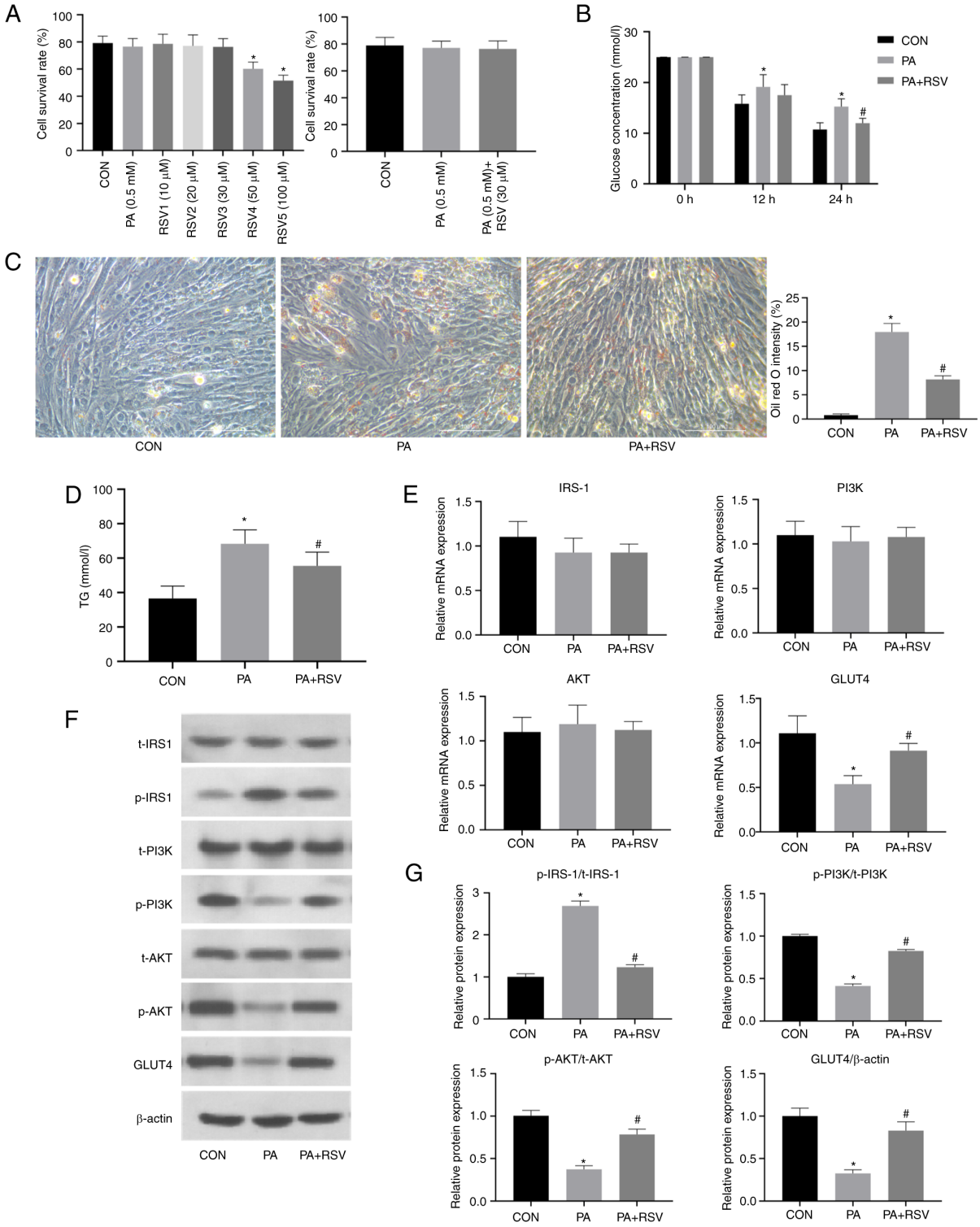

Figure 2. RSV alleviates PA-induced lipid deposition and insulin resistance in C2C12 cells. (A) Survival rates of C2C12 cells after treatment with PA and RSV. (B) Glucose concentration in the culture medium was decreased after RSV treatment for 24 h. (C) Lipid deposition was decreased in Oil red O-stained C2C12 cells after RSV treatment; magnification, x400, scale bar, 100 μm. (D) TG content in C2C12 cells was decreased after RSV treatment. (E) Effects of RSV treatment on the mRNA expression levels of insulin pathway indicators in C2C12 cells. (F) Effects of RSV treatment on the protein expression levels of insulin pathway indicators in C2C12 cells after RSV treatment. (G) Semi-quantification of p-protein/t-protein ratios for insulin pathway indicators and protein expression levels of GLUT4 in C2C12 cells after RSV treatment. All cells were treated with 100 nM insulin for 30 min before (B) detection of glucose contents and (F) western blotting. Data are presented as the mean ± SD (n=3). *P<0.05 vs. CON, $^{\#}$P<0.05 vs. PA. CON, control; RSV, resveratrol; PA, palmitic acid; IRS-1, insulin receptor substrate-1; GLUT4, glucose transporter 4; p-, phosphorylated; t-t, total; TG, triglyceride.

(Fig. 4F), and the p-protein/t-protein ratios were also increased (Fig. 4G). These findings indicated that silencing DDIT4 reversed the attenuating effects of RSV on the increased p-protein/t-protein ratios for mTOR and p70S6K following PA treatment, thus suggesting that RSV inhibited the mTOR pathway through DDIT4.

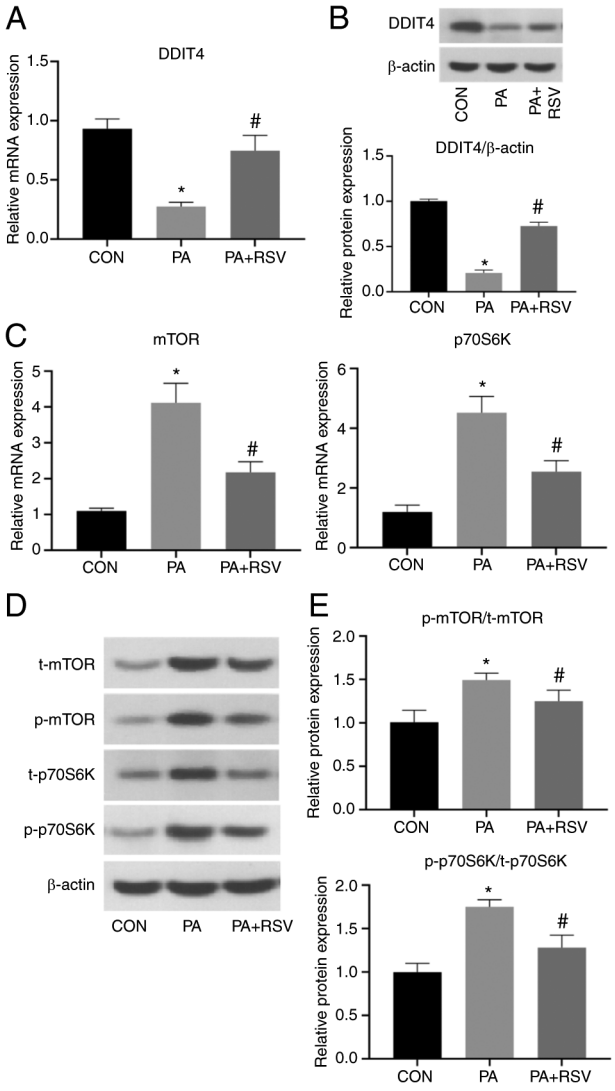

Figure 3. Effects of RSV on DDIT4 and mTOR pathway indicators in C2C12 cells with PA-induced insulin resistance. (A) mRNA and (B) protein expression levels of DDIT4 in C2C12 cells was increased after RSV treatment. (C) mRNA and (D) protein expression levels of mTOR pathway indicators in C2C12 cells were decreased after RSV treatment. (E) Semi-quantification of p-protein/t-protein ratios for mTOR pathway indicators, which were decreased after RSV treatment. (B and D) All cells were treated with 100 nM insulin for 30 min before western blotting. Data are presented as the mean ± SD (n=3). *P<0.05 vs. CON, $^{\#}$P<0.05 vs. PA. CON, control; RSV, resveratrol; PA, palmitic acid; DDIT4, DNA damage-inducible transcript 4; p70S6K, p70 ribosomal protein S6 kinase; p-, phosphorylated; t-t, total.

Compared with in the PA + RSV group, the protein expression levels of p-PI3K/t-PI3K, p-AKT/t-AKT and GLUT4 were decreased, whereas the protein expression levels of p-IRS-1/t-IRS-1 were increased in the PA + RSV + DDIT4-siRNA group after silencing of DDIT4 (Fig. 4H and I). None of the treatments affected the total protein expression levels of PI3K, AKT and IRS-1. These results indicated that DDIT4 served a positive role in RSV-mediated improvement of PA-induced IR.

Expression of DDIT4, mTOR and insulin signaling pathways markers in MHY1485-treated C2C12 cells. Compared with in the PA + RSV group, the glucose concentration was significantly increased in the culture medium from the PA + RSV + MHY1485 group, which offset the effect of RSV (Fig. 5A). These findings indicated that mTOR activation may weaken the beneficial effect of RSV on glucose metabolism.

In terms of lipid metabolism, the Oil red O-stained lipid droplets and TG content in the cells were increased in the PA + RSV + MHY1485 group compared with those in the PA + RSV group (Fig. 5B and C), indicating that activation of the mTOR pathway reduced the effect of RSV on improving cellular lipid deposition.

Notably, there were no differences in the mRNA and protein expression levels of DDIT4 between the PA + RSV + MHY1485 group and the PA + RSV group (Fig. 5D-F), suggesting that MHY1485 did not affect the expression of DDIT4. Compared with in the PA + RSV group, the t-protein and p-protein expression levels for mTOR and p70S6K were increased in the PA + RSV + MHY1485 group, and the p-protein/t-protein ratios for mTOR and p70S6K were also increased (Fig. 5E and F), indicating that MHY1485 increased the mTOR pathway activity and counteracted the inhibitory effect of RSV on the mTOR pathway.

Compared with in the PA + RSV group, the protein expression levels of p-PI3K/t-PI3K, p-AKT/t-AKT and GLUT4 were downregulated in the PA + RSV + MHY1485 group, whereas the protein expression levels of p-IRS-1/t-IRS-1 were upregulated (Fig. 5G and H). These findings indicated that activation of the mTOR pathway may weaken the effect of RSV and lead to IR. The results of the present study revealed that RSV could inhibit the mTOR pathway by increasing DDIT4, thereby improving PA-induced IR and lipid deposition in C2C12 cells (Fig. 6).

Discussion

RSV, a plant-derived compound, has the potential to improve IR, a focus of numerous research groups. RSV has been reported to alleviate IR in high-fructose corn syrup-fed rats (27), improve IR in hyperlipidemic mice and obese Zucker rats (28), improve abnormal liver glucose metabolism induced by high-fat diet intake through adenosine 5'-monophosphate-activated protein kinase pathway (29), and upregulate mmu-microRNA-363-3p through the PI3K/AKT pathway to improve high-fat diet-induced IR in mice (30). RSV is an anti-diabetic drug that warrants further research. In our previous study, high-throughput sequencing showed that DDIT4 mRNA expression was decreased in the skeletal muscle of high-fat diet-fed mice, and was increased following treatment of these mice with RSV (31).

The present study established a PA-induced IR model in C2C12 cells and used this model to study the effects of RSV on improving IR *in vitro*. The concentration of RSV used was 30 μM, because 10 and 20 μM RSV had no significant effect on cell survival rate, whereas 50 and 100 μM RSV significantly reduced the cell survival rate. In a previous study from our group, RSV treatment was found to improve IR and lipid deposition in the skeletal muscle cells of high-fat diet-fed mice and PA-treated L6 rats (32). In the present study, RSV was found to reverse the effect of PA on C2C12 cells, upregulate the expression of DDIT4, inhibit the mTOR/P70S6K pathway, reduce the expression of p-IRS-1, increase the expression levels of p-PI3K and p-Akt in the insulin pathway, activate the expression of GLUT4, promote glucose uptake, reduce lipid

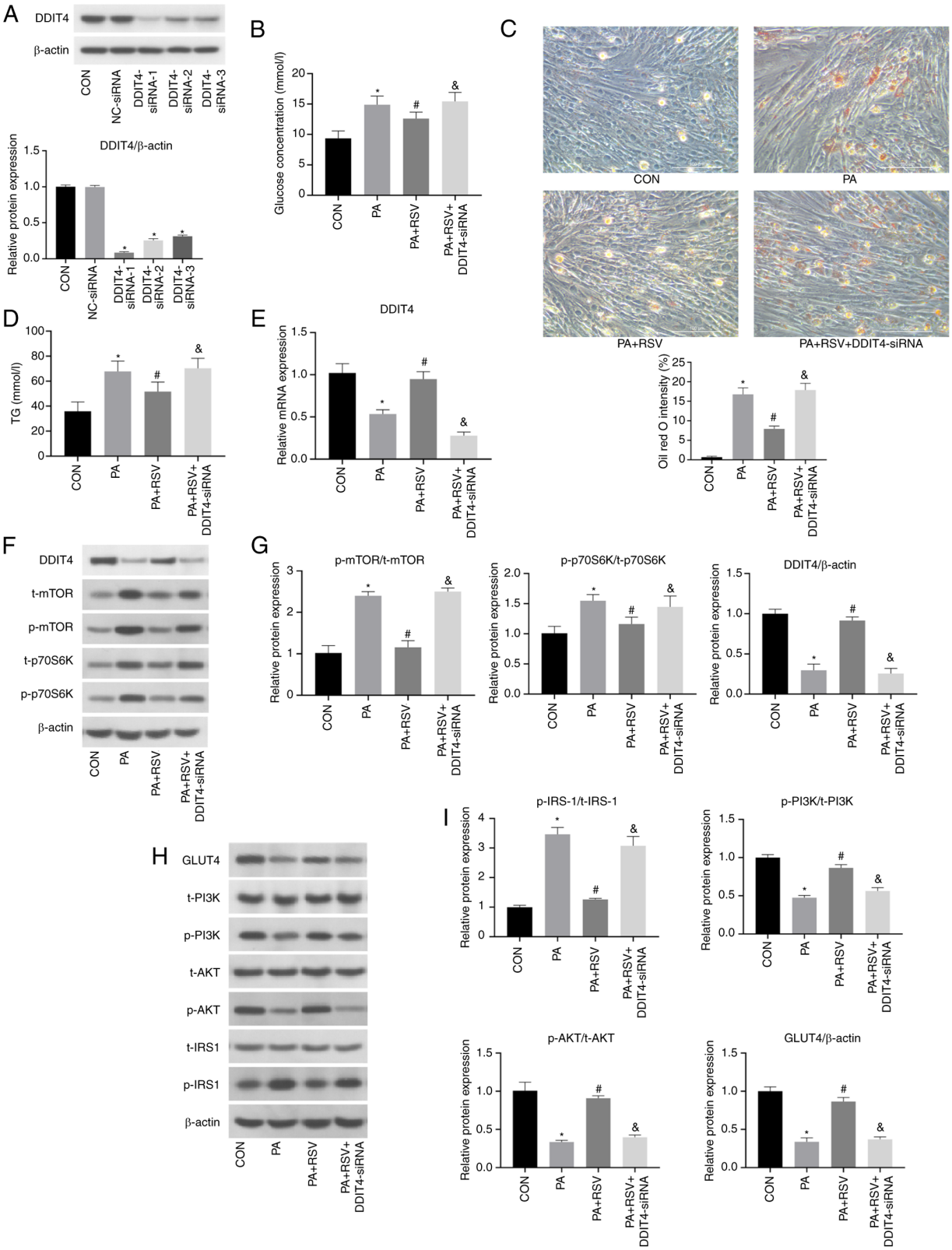

Figure 4. Expression levels of insulin signaling pathway and mTOR pathway indicators after silencing of DDIT4 in C2C12 cells with PA-induced insulin resistance. (A) Protein expression levels of DDIT4 were decreased after transfection with three DDIT4-siRNAs. (B) Glucose concentration in the culture medium of C2C12 cells was increased after silencing DDIT4. (C) Number of red lipid droplets in C2C12 cells was increased after silencing DDIT4, as determined by Oil red O staining; magnification, x400, scale bar, 100 μm. (D) TG levels in C2C12 cells were increased after silencing DDIT4. (E) mRNA expression levels of DDIT4 were decreased after silencing DDIT4. (F) Protein expression levels of DDIT4 and mTOR pathway indicators after silencing DDIT4. (G) Semi-quantification of p-protein/t-protein ratios for mTOR pathway indicators and protein expression levels of DDIT4 after silencing DDIT4. (H) Protein expression levels of insulin signaling pathway indicators after silencing of DDIT4. (I) Semi-quantification of p-protein/t-protein ratios for insulin signaling pathway indicators and protein expression levels of GLUT4 after silencing of DDIT4. All cells were treated with 100 nM insulin for 30 min before (B) detection of glucose contents and (A, F and H) western blotting. Data are presented as the mean ± SD (n=3). *P<0.05 vs. CON, $^{\#}$P<0.05 vs. PA, $^{\&}$P<0.05 vs. PA + RSV. CON, control; RSV, resveratrol; PA, palmitic acid; siRNA, small interfering RNA; NC, negative control; DDIT4, DNA damage-inducible transcript 4; p70S6K, p70 ribosomal protein S6 kinase; IRS-1, insulin receptor substrate-1; GLUT4, glucose transporter 4; p-, phosphorylated; t-t, total; TG, triglyceride.

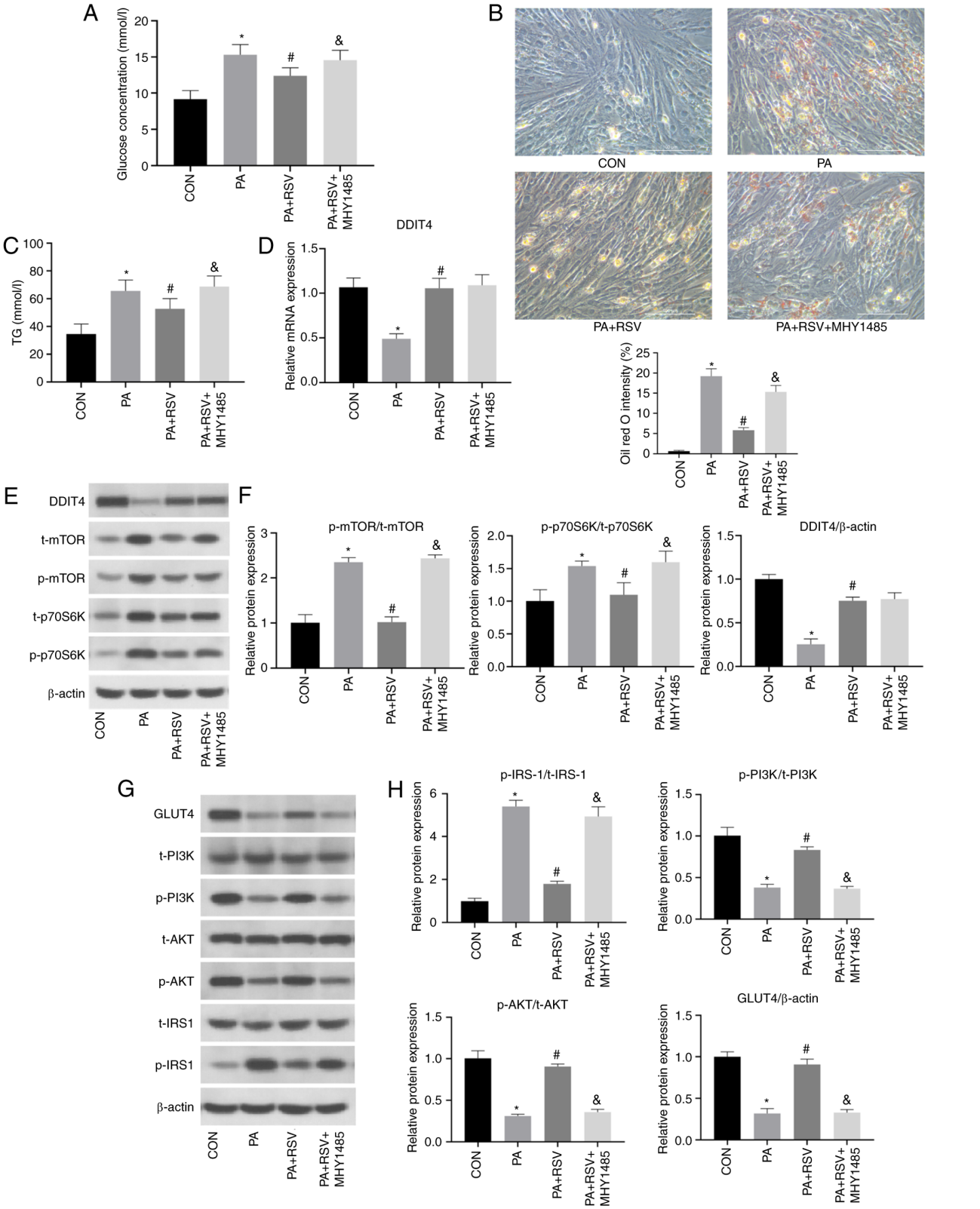

Figure 5. Expression levels of indicators related to the DDIT4, mTOR and insulin signaling pathways in MHY1485-treated C2C12 cells with PA-induced insulin resistance. (A) Glucose concentration in the culture medium of C2C12 cells was increased after activation of mTOR. (B) Number of red lipid droplets in C2C12 cells was increased after activation of mTOR, as determined by Oil red O staining; magnification, x400, scale bar, 100 μm. (C) TG content in C2C12 cells was increased after activation of mTOR. (D) mRNA expression levels of DDIT4 after activation of mTOR. (E) Protein expression levels of DDIT4 and mTOR signaling pathway indicators after activation of mTOR. (F) Semi-quantification of p-protein/t-protein ratios for mTOR signaling pathway indicators and protein expression levels of DDIT4 after activation of mTOR. (G) Protein expression levels of insulin signaling pathway indicators after activation of mTOR. (H) Semi-quantification of p-protein/t-protein ratios for insulin signaling pathway indicators and protein expression levels of GLUT4 after activation of mTOR. All cells were treated with 100 nM insulin for 30 min before (A) detection of glucose contents and (E and G) western blotting. Data are presented as the mean ± SD (n=3). *P<0.05 vs. CON, $^{\#}$P<0.05 vs. PA, $^{\&}$P<0.05 vs. PA + RSV. CON, control; RSV, resveratrol; PA, palmitic acid; DDIT4, DNA damage-inducible transcript 4; p70S6K, p70 ribosomal protein S6 kinase; IRS-1, insulin receptor substrate-1; GLUT4, glucose transporter 4; p-, phosphorylated; t-t, total; TG, triglyceride.

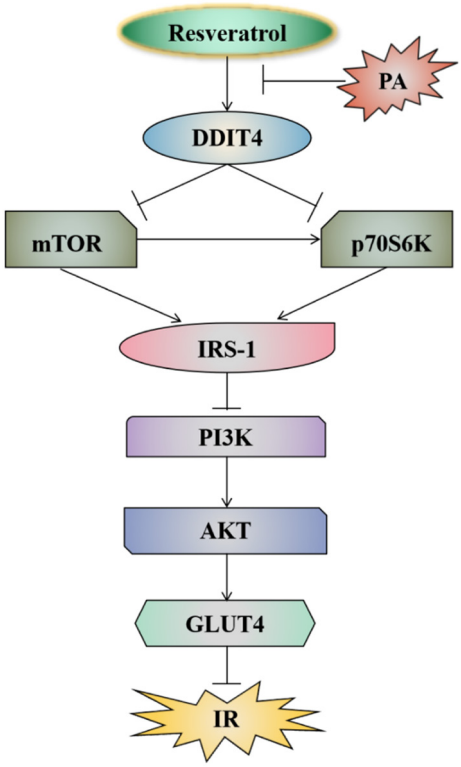

Figure 6. Resveratrol ameliorates insulin resistance by improving insulin signaling via the DDIT4/mTOR/IRS-1/PI3K/AKT/GLUT4 pathway. IR, insulin resistance; PA, palmitic acid; DDIT4, DNA damage-inducible transcript 4; p70S6K, p70 ribosomal protein S6 kinase; IRS-1, insulin receptor substrate-1; GLUT4, glucose transporter 4.

deposition and alleviate PA-induced IR in C2C12 myocyte cells. After silencing DDIT4 by DDIT4-siRNA transfection or activating mTOR by MHY1485 treatment, the beneficial effects of RSV on improving IR, and glucose and lipid metabolism were significantly attenuated. These results indicated that RSV could inhibit the mTOR/p70S6K signaling pathway activity through activation of DDIT4, thereby improving IRS-1/PI3K/AKT/GLUT4 insulin signaling and significantly alleviating IR, and improving glucose and lipid metabolism.

DDIT4 is a potent mTOR inhibitor (33) involved in DNA damage repair, growth during hypoxia, cell stress and other effects (34-36). DDIT4 has been shown to inhibit the mTOR pathway and improve insulin pathway signaling, whereas DDIT4 deficiency can increase systemic glucose and promote IR, and impair skeletal muscle insulin signaling (37). Sustained DDIT4 overexpression has been shown to inhibit mTOR activity in a tuberous sclerosis complex 1/2 (TSC1/2)-mediated manner, with significantly reduced levels of p-p70S6K and induction of AKT phosphorylation at serine 473, whereas rapamycin-mediated mTOR inhibition increases the phosphorylation level of AKT (38). High glucose can inhibit DDIT4 and TSC1/2 in β-cells, upregulate Ras homolog enriched in brain/mTOR/p70S6K, and enhance the expression of apoptosis-regulating proteins (39). Furthermore, 1,25$(OH)_2$D3 can activate the expression of DDIT4 in the renal tissue of diabetic rats, reduce the expression of p-mTOR and p-p70S6K, promote the downstream insulin pathway activity, inhibit the proliferation of rat mesangial cells induced by high glucose, and improve the glucose and lipid metabolism in diabetic rats (40,41). Other studies have shown that activation of the mTOR/p70S6K signaling pathway is a physiological feedback mechanism for insulin-stimulated glucose transport in skeletal muscle cells, leading to aberrant serine/tyrosine phosphorylation of IRS-1 (19,42). Further studies have confirmed that the attenuation of free fatty acid-induced IR in skeletal muscle cells by RSV is closely related to the inhibition of mTOR and p70S6K (43). In the present study, with the aim of further clarifying the underlying mechanism for the involvement of the DDIT4/mTOR pathway in the improvement of IR by RSV, DDIT4 was silenced by DDIT4-siRNA transfection and the mTOR pathway was activated by MHY1485 treatment, after which, the effects of RSV on improving glucose utilization and IR were weakened. The results further revealed that RSV increased DDIT4 expression, inhibited mTOR and p70S6K activation, increased the expression of IRS-1/PI3K/AKT/GLUT4 insulin pathway indicators, and promoted insulin signaling transduction and glucose uptake, which may comprise one of the mechanisms for the RSV-mediated improvement in skeletal muscle IR. However, a limitation of the present study is that the mechanism was verified only in skeletal muscle cells *in vitro*. We aim to further explore the relationship between RSV and the DDIT4/mTOR pathway *in vivo* using an animal model.

In conclusion, the present study confirmed that RSV could inhibit the mTOR/p70S6K pathway by increasing the expression of DDIT4, thereby ameliorating IR and alleviating lipid deposition in C2C12 cells.

Acknowledgements

Not applicable.

Funding

This study was partially supported by the Scientific Research Project of Hebei Provincial Administration of Traditional Chinese Medicine (grant no. 2023010).

Availability of data and materials

The datasets used and/or analyzed during the current study are available from the corresponding author on reasonable request.

Authors' contributions

XP and GS conceived and designed the study. XP, CL, XW, MZ, ZZ, XZ and CW acquired and analyzed the data. XP, CW and GS confirm the authenticity of all the raw data. XP prepared the draft of the manuscript. All authors read and approved the final manuscript.

Ethics approval and consent to participate

Not applicable.

Patient consent for publication

Not applicable.

Competing interests

The authors declare that they have no competing interests.

References

1. Wang Y, Yang LZ, Yang DG, Zhang QY, Deng ZN, Wang K and Mao XJ: MiR-21 antagomir improves insulin resistance and lipid metabolism disorder in streptozotocin-induced type 2 diabetes mellitus rats. Ann Palliat Med 9: 394-404, 2020.
2. Fernandes GW and Bocco BMLC: Hepatic mediators of lipid metabolism and ketogenesis: Focus on fatty liver and diabetes. Curr Diabetes Rev 17: e110320187539, 2021.
3. Petersen MC and Shulman GI: Mechanisms of insulin action and insulin resistance. Physiol Rev 98: 2133-2223, 2018.
4. Merz KE and Thurmond DC: Role of skeletal muscle in insulin resistance and glucose uptake. Compr Physiol 10: 785-809, 2020.
5. Houzelle A, Jörgensen JA, Schaart G, Daemen S, van Polanen N, Fealy CE, Hesselink MKC, Schrauwen P and Hoeks J: Human skeletal muscle mitochondrial dynamics in relation to oxidative capacity and insulin sensitivity. Diabetologia 64: 424-436, 2021.
6. Robertson I, Wai Hau T, Sami F, Sajid Al M, Badgujar V, Murtuja S, Saquib Hasnain M, Khan A, Majeed S and Tahir Ansari M: The science of resveratrol, formulation, pharmacokinetic barriers and its chemotherapeutic potential. Int J Pharm 618: 121605, 2022.
7. Su M, Zhao W, Xu S and Weng J: Resveratrol in treating diabetes and its cardiovascular complications: A review of its mechanisms of action. Antioxidants (Basel) 11: 1085, 2022.
8. Mongioì LM, La Vignera S, Cannarella R, Cimino L, Compagnone M, Condorell RA and Calogero AE: The role of resveratrol administration in human obesity. Int J Mol Sci 22: 4362, 2021.
9. Barber TM, Kabisch S, Randeva HS, Pfeiffer AFH and Weickert MO: Implications of resveratrol in obesity and insulin resistance: A state-of-the-art review. Nutrients 14: 2870, 2022.
10. Kang BB and Chiang BH: Amelioration of insulin resistance using the additive effect of ferulic acid and resveratrol on vesicle trafficking for skeletal muscle glucose metabolism. Phytother Res 34: 808-816, 2020.
11. Abo Alrob O, Al-Horani RA, Altaany Z and Nusair MB: Synergistic beneficial effects of resveratrol and diet on high-fat diet-induced obesity. Medicina (Kaunas) 58: 1301, 2022.
12. Meng Q, Li J, Wang C and Shan A: Biological function of resveratrol and its application in animal production: A review. J Anim Sci Biotechno 14: 25, 2023.
13. Shahwan M, Alhumaydhi F, Ashraf GM, Hasan PMZ and Shamsi A: Role of polyphenols in combating type 2 diabetes and insulin resistance. Int J Biol Macromol 206: 567-579, 2022.
14. Koundouros N and Blenis J: Targeting mTOR in the context of diet and whole-body metabolism. Endocrinology 163: bqac041, 2022.
15. Fan H, Wu Y, Yu S, Li X, Wang A, Wang S, Chen W and Lu Y: Critical role of mTOR in regulating aerobic glycolysis in carcinogenesis (review). Int J Oncol 58: 9-19, 2021.
16. Rapaka D, Bitra VR, Challa SR and Adiukwu PC: mTOR signaling as a molecular target for the alleviation of Alzheimer's disease pathogenesis. Neurochem Int 155: 105311, 2022.
17. Ong PS, Wang LZ, Dai X, Tseng SH, Loo SJ and Sethi G: Judicious toggling of mTOR activity to combat insulin resistance and cancer: Current evidence and perspectives. Front Pharmacol 7: 395, 2016.
18. Pan S, Lin H, Luo H, Gao F, Meng L, Zhou C, Jiang C, Guo Y, Ji Z, Chi J and Guo H: Folic acid inhibits dedifferentiation of PDGF-BB-induced vascular smooth muscle cells by suppressing mTOR/P70S6K signaling. Am J Transl Res 9: 1307-1316, 2017.
19. Faheem and Sivasubrmanian S: Fathoming the role of mTOR in diabetes mellitus and its complications. Curr Mol Pharmacol 16: 520-529, 2023.
20. Hayasaka M, Tsunekawa H, Yoshinaga M and Murakami T: Endurance exercise induces REDD1 expression and transiently decreases mTORC1 signaling in rat skeletal muscle. Physiol Rep 2: e12254, 2014.
21. Gordon BS, Williamson DL, Lang CH, Jefferson LS and Kimball SR: Nutrient-induced stimulation of protein synthesis in mouse skeletal muscle is limited by the mTORC1 repressor REDD1. J Nutr 145: 708-713, 2015.
22. Lipina C and Hundal HS: Is REDD1 a metabolic éminence grise? Trends Endocrinol Metab 27: 868-880, 2016.
23. DeYoung MP, Horak P, Sofer A, Sgroi D and Ellisen LW: Hypoxia regulates TSC1/2-mTOR signaling and tumor suppression through REDD1-mediated 14-3-3 shuttling. Genes Dev 22: 239-251, 2008.
24. Regazzetti C, Dumas K, Le Marchand-Brustel Y, Peraldi P, Tanti JF and Giorgetti-Peraldi S: Regulated in development and DNA damage responses-1 (REDD1) protein contributes to insulin signaling pathway in adipocytes. PLoS One 7: e52154, 2012.
25. Shengchen W, Jing L, Yujie Y, Yue W and Shiwen X: Polystyrene microplastics-induced ROS overproduction disrupts the skeletal muscle regeneration by converting myoblasts into adipocytes. J Hazard Mater 417: 125962, 2021.
26. Livak KJ and Schmittgen TD: Analysis of relative gene expression data using real-time quantitative PCR and the 2(-Delta Delta C(T)) method. Methods 25: 402-408, 2001.
27. Babacanoglu C, Yildirim N, Sadi G, Pektas MB and Akar F: Resveratrol prevents high-fructose corn syrup-induced vascular insulin resistance and dysfunction in rats. Food Chem Toxicol 60: 160-167, 2013.
28. Sung MM, Kim TT, Denou E, Soltys CM, Hamza SM, Byrne NJ, Masson G, Park H, Wishart DS, Madsen KL, *et al*: Improved glucose homeostasis in obese mice treated with resveratrol is associated with alterations in the gut microbiome. Diabetes 66: 418-425, 2017.
29. Lu C, Xing H, Yang L, Chen K, Shu L, Zhao X and Song G: Resveratrol ameliorates high-fat-diet-induced abnormalities in hepatic glucose metabolism in mice via the AMP-activated protein kinase pathway. Evid Based Complement Alternat Med 2021: 6616906, 2021.
30. Shu L, Zhao H, Huang W, Hou G, Song G and Ma H: Resveratrol upregulates mmu-miR-363-3p via the PI3K-Akt pathway to improve insulin resistance induced by a high-fat diet in mice. Diabetes Metab Syndr Obes 13: 391-403, 2020.
31. Liu Z, Zhang Z, Song G, Wang X, Xing H and Wang C: Resveratrol alleviates skeletal muscle insulin resistance by downregulating long noncoding RNA. Int J Endocrinol 2022: 2539519, 2020.
32. Zhang YJ, Zhao H, Dong L, Zhen YF, Xing HY, Ma HJ and Song GY: Resveratrol ameliorates high-fat diet-induced insulin resistance and fatty acid oxidation via ATM-AMPK axis in skeletal muscle. Eur Rev Med Pharmacol Sci 23: 9117-9125, 2019.
33. Dennis MD, Coleman CS, Berg A, Jefferson LS and Kimball SR: REDD1 enhances protein phosphatase 2A-mediated dephosphorylation of Akt to repress mTORC1 signaling. Sci Signal 7: ra68, 2014.
34. Ellisen LW, Ramsayer KD, Johannessen CM, Yang A, Beppu H, Minda K, Oliner JD, McKeon F and Haber DA: REDD1, a developmentally regulated transcriptional target of p63 and p53, links p63 to regulation of reactive oxygen species. Mol Cell 10: 995-1005, 2002.
35. Shoshani T, Faerman A, Mett I, Zelin E, Tenne T, Gorodin S, Moshel Y, Elbaz S, Budanov A, Chajut A, *et al*: Identification of a novel hypoxia-inducible factor 1-responsive gene, RTP801, involved in apoptosis. Mol Cell Biol 22: 2283-2293, 2002.
36. Wang Z, Malone MH, Thomenius MJ, Zhong F, Xu F and Distelhorst CW: Dexamethasone-induced gene 2 (dig2) is a novel pro-survival stress gene induced rapidly by diverse apoptotic signals. J Biol Chem 278: 27053-27058, 2003.
37. Dungan CM, Wright DC and Williamson DL: Lack of REDD1 reduces whole body glucose and insulin tolerance, and impairs skeletal muscle insulin signaling. Biochem Biophys Res Commun 453: 778-783, 2014.
38. Jin HO, Hong SE, Kim JH, Choi HN, Kim K, An S, Choe TB, Hwang CS, Lee JH, Kim JI, *et al*: Sustained overexpression of Redd1 leads to Akt activation involved in cell survival. Cancer Lett 336: 319-324, 2013.
39. Yang Z, Liu F, Qu H, Wang H, Xiao X and Deng H: 1, 25$(OH)_2$D3 protects β cell against high glucose-induced apoptosis through mTOR suppressing. Mol Cell Endocrinol 414: 111-119, 2015.
40. Chen DP, Ma YP, Zhuo L, Zhang Z, Zou GM, Yang Y, Gao HM and Li WG: 1,25-Dihydroxyvitamin D_3 inhibits the proliferation of rat mesangial cells induced by high glucose via DDIT4. Oncotarget 9: 418-427, 2017.
41. Wang H, Wang J, Qu H, Wei H, Ji B, Yang Z, Wu J, He Q, Luo Y, Liu D, *et al*: In vitro and in vivo inhibition of mTOR by 1,25-dihydroxyvitamin D_3 to improve early diabetic nephropathy via the DDIT4/TSC2/mTOR pathway. Endocrine 54: 348-359, 2016.
42. Vlavcheski F and Tsiani E: Attenuation of free fatty acid-induced muscle insulin resistance by rosemary extract. Nutrients 10: 1623, 2018.
43. Den Hartogh DJ, Vlavcheski F, Giacca A and Tsiani E: Attenuation of free fatty acid (FFA)-induced skeletal muscle cell insulin resistance by resveratrol is linked to activation of AMPK and inhibition of mTOR and p70S6K. Int J Mol Sci 21: 4900, 2020.